Closely interleaved self-comparison method applied to precise measurement

Fan Zou (邹 凡)[1,2], Rong Wei (魏 荣)[1,*], Richang Dong (董日昌)[1,2], Tingting Chen (陈婷婷)[1,2], Wenli Wang (王文丽)[1], and Yuzhu Wang (王育竹)[1]

[1]*Key Laboratory of Quantum Optics, Shanghai Institute of Optics and Fine Mechanics, Chinese Academy of Sciences, Shanghai 201800, China*

[2]*University of Chinese Academy of Sciences, Beijing 100049, China*

**Corresponding author: weirong@siom.ac.cn*

Received February 18, 2016; accepted May 24, 2016; posted online June 30, 2016

A self-comparison method with closely interleaved switching states is analyzed and used to evaluate some type-B uncertainties of an ^{87}Rb atomic fountain clock. Free from additional frequency reference, the method can be applied to a running fountain to reach a precision beyond its uncertainty. A verification experiment proves an uncertainty of 9.2×10^{-16} at an averaging time of 242500 s. Further, the method is applied to measure light shift, and no visible relative frequency shift is found in the fountain within the uncertainty of 2.1×10^{-15}. When applied to the evaluation of a cold collisional shift, the result gives a -2.2×10^{-15} shift with a 9.5×10^{-16} uncertainty.

OCIS codes: 020.1335, 120.3940.

doi: 10.3788/COL201614.081201.

As the most active field of time and frequency standards, atomic fountain clocks and optical clocks have shown great importance in the definition of the Système International (SI) second[1], timing applications[2], and numerous precise measurements[3,4]. Over several decades of development, ^{133}Cs and ^{87}Rb atomic fountain clocks have achieved a 1.1×10^{-16} uncertainty[5] with a few parts in a 1×10^{17} instability[2]. Additionally, with frequencies more than five orders higher and instabilities much lower than that of fountain clocks, optical clocks sparked interest in the last ten years. Recently, an Sr optical lattice clock with a 1×10^{-18} level of uncertainty has been demonstrated[6]. Similar results are also realized in a Yb lattice clock[7], Al^+ ion clock[8], and so on. Among these triumphs in achieving unprecedented uncertainties and instabilities of atomic clocks, the systematic evaluation of type-B uncertainties, including cold atom collisional frequency shift and light shift[1,5], etc., is critical because it not only determines the performance of a specific clock, but also illustrates the potential improvements that one could strive for. This evaluation, as the central issue of clocks, has been consistently contributing to the improved determination of clock performance.

Generally, type-B uncertainties can be obtained by either direct evaluation or indirect evaluation. In direct evaluation, uncertainties are given by the comparison of frequency errors of the clock running in different states. In indirect evaluation, only the fluctuations of physical parameters are recorded, and then used to calculate the physical effects. Preference usually lies on direct evaluation because it has better credibility, especially for major effects in clocks. Furthermore, in pursuit of better determination of type-B uncertainties with a particularly small effect and uncertainties hard to obtain directly, the self-comparison method, as a direct evaluation, is widely used. The self-comparison is fulfilled by the same clock running in different states[1,6,9–16]. Since the method is significant in the removal of systematic errors, it has succeeded in the evaluation of cold collisional frequency shifts of ^{133}Cs and ^{87}Rb atomic fountain clocks[1,9,10]. Besides, self-comparison is also used in the evaluation of optical lattice clocks, partially due to the lack of comparable clocks[6,11–16].

On the basis of the widely used self-comparison method, a closely interleaved self-comparison (CISC) method has been put forward to further suppress the systematic errors and potential long-term drifts. The method switches the clock between two states to obtain corresponding error signals. These error signals are used to calculate the relative frequency shift of the physical effect. Our CISC method can bypass the reference clock and extra comparison loops required in other methods[1,9,10], and leads to better applicability for high precise clocks. The method can also evaluate the uncertainties without interrupting the running of the clock, and provides more information for the Allan deviation at short averaging times due to the close interleaving. Furthermore, to demonstrate the validity of CISC method, the relationships between instability and related noise are analyzed. The Allan deviation is adopted to characterize the instabilities because it provides a clear dependence of the deviation on the averaging time, and it is convergent for most types of clock noise[17]. A $\tau^{-1/2}$ time dependence of the Allan deviation in CISC is predicted. Then, the CISC is applied to the type-B uncertainty evaluation of the ^{87}Rb atomic fountain clock at the Shanghai Institute of Optics and Fine Mechanics (SIOM). The results verify that CISC is able to break the instability limit set by the inter-clock comparison.

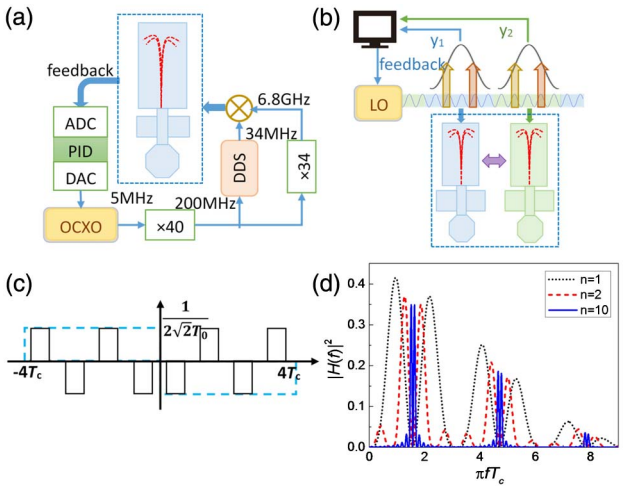

Fig. 1. (a) LO locking scheme, where 6.834 682 ..... GHz with ±0.5 Hz modulation is multiplied from a 5 MHz OCXO oscillator and delivered to the fountain. The feedback signal is directly applied to the OCXO oscillator every two launch cycles to lock its frequency to the resonance spectra of ^{87}Rb atoms. (b) CISC scheme with atomic fountain switching between two states with different sets of parameters. Error signals from the two states are recorded to lock the LO and used to identify the frequency difference of the two states. (c) Transfer function in time domain where the averaging time is $4T_c$. The blue line is the case in a normal Allan variance, while the black line is the case in CISC with extra modulation on the effect of interest. (d) Frequency conjugate of the transfer function with different averaging times, which are determined by $2nT_c$.

As described in our previous works[18–21], an ^{87}Rb atomic fountain clock at the SIOM has locked its local oscillator (LO) to the resonance spectra of hyperfine transition of the ^{87}Rb ground level. The LO locking scheme depicted in Fig. 1(a) is the basis of the evaluation of type-B uncertainties using the CISC method. In our fountain, about 1×10^8 atoms are trapped, cooled, and launched. Subjected to gravity, atoms interact with the microwave twice in a Ramsey cavity. Via modulating the frequency multiplied from an oven controlled crystal oscillator (OCXO) to both sides at full width at half-maximum of the center Ramsey fringe, feedback signals are obtained and applied to the OCXO every two launch cycles. Thus, the output of the LO follows the characteristics of the fountain, and a $2.7\times10^{-13}\ \tau^{-1/2}$ instability[19] is achieved by our fountain system.

Challenged by the dilemma of lacking comparable clocks and the problem that effects such as cold collisional shift cannot be easily obtained by indirect evaluation, we propose a CISC method as illustrated by Fig. 1(b) to promote the evaluation of type-B uncertainties. In this method, the clock is switched every two launch cycles between two states with different values of the effect of interest, for example the atom density, microwave power in the Ramsey cavity, the stray light during the Ramsey interrogation, and so on. Through proper switching, the state of the clock is actually modulated considering the effect of interest. The different scales of effects lead to different transition probabilities of atoms, and thus, the calculated frequency shifts refer to the atom hyperfine resonance frequency. The calculated frequency shifts are recorded as the error signals, which also contain different scales of the effect. Along with this modulation of clock states, two adjacent error signals y_1 and y_2 from two different states switched in the clock are utilized to lock the LO after program processing. Consequently, it typically requires four launch cycles to lock the LO rather than the two launch cycles in the LO locking scheme in Fig. 1(a). Meanwhile, the differential error signals y_2-y_1 between adjacent cycles are used to calculate the frequency shift due to the effect. In other words, the single clock can be viewed as two identical clocks with all the same parameters except for the one switched in the CISC method. The differential error signals y_2-y_1 reflect the systematic bias due to the effect, and the comparison involved the noises from the two clocks.

The instabilities of atomic clocks are highly related to the structure of the clock and the power spectral density (PSD) of the noise of its relative frequency shifts. The PSD could be decomposed into the superposition of five independent noise processes, i.e., $S(f)=\sum_{\alpha=-2}^{2}h_\alpha f^\alpha$[17]. Since the CISC scheme has distinct timing and treatment of error signals compared with the LO locking scheme, the noise from the LO will lead to different results. In the LO locking scheme, the error signals are fed back to the LO to ensure continuous frequency output, the result of which is the reduced noise of the LO except for white noise. Yet, the evaluation of the clock given by the comparison to a reference clock, namely an inter-clock comparison between a hydrogen maser and atomic fountain, is affected by all types of noises from both clocks. However, if the reference clock is removed as in the CISC, the result would be unrelated to the noise of the reference clock.

For the evaluation using CISC, the differential error signals y_2-y_1 are used to describe the effect of interest. In this case by converting noise from the frequency domain into the Allan variance[17] in the time domain and taking into account the self-comparison process that the error signals are actually positively or negatively modulated within the normal Allan variance, it can easily lead to a transfer function $h(t)=\sum_{m=1}^{n}h_m(t)$, in which

$$h_m(t)=\begin{cases}\frac{(-1)^m}{\sqrt{2}nT_c} & [(m-1)T_c+t_0,\,mT_c-t_0]\\ 0 & [-mT_c+t_0,\,-(m-1)T_c-t_0]\\ & \text{otherwise}\end{cases},\quad(1)$$

and its Fourier conjugate

$$|H(f)|^2=\frac{2\sin^2(\pi fT_0)\sin^4(2n\pi fT_c)}{(n\pi fT_c)^2\cos^2(\pi fT_c)},\quad(2)$$

which represents the hypothetical filter act on error signals y_1 and y_2. The transfer function and its Fourier conjugate are depicted in Figs. 1(c) and 1(d). In Eqs. (1) and (2), T_0 is the time of atom interrogation, $t_0=\frac{T_c-T_0}{2}$,

T_c is twice the launch cycle, n is the number of cycles that the effect is switched, and m denotes the m-th component of the transfer function. The averaging time is determined by $\tau = 2nT_c$. Note that when $f = \frac{1}{T_c}(\frac{1}{2} + k)$ and k is an integer, $H(f)$ in Eq. (2) should actually be the limit at these undefined points. Therefore, the PSD $S_y(f)$ of the error signals filtered by $|H(f)|^2$ will, consequently, lead to the Allan variance $\sigma_y^2(\tau) = \int_0^\infty |H(f)|^2 S_y(f) \mathrm{d}f$[17] in the CISC scheme. Specifically, if the dead time is not considered, the integral of the PSD component with $\alpha = 0$ (i.e., white frequency noise, WFM) and $\alpha = -2$ (i.e., random walk of frequency noise, RWFM) contributes $\frac{2h_0}{\tau}$ and $\frac{8\pi^2 T_c^2 h_{-2}}{3\tau}$ to the Allan variance, respectively. But in the inter-clock comparison, RWFM would make a contribution with $\tau^{1/2}$ dependence to the Allan deviation[17]. In CISC, The $\tau^{-1/2}$ dependence of the Allan deviation suggests that the RWFM component of the PSD acts as WFM in the CISC scheme, and the same can be applied on flick frequency noise (FFM), which normally leads to an instability floor in the inter-clock comparison[17].

By switching an ^{87}Rb atomic fountain between two identical states, the CISC is confirmed to have a $\tau^{-1/2} = (nT_c)^{-1/2}$ dependence in the Allan deviation, which is shown as the black solid line in Fig. 2(a). Meanwhile, a comparison between the fountain and a hydrogen maser (VCH-1003 A) scales, shown as the red dashed line, which increases at averaging time longer than 1×10^4 s. The comparison in the CISC is $\sqrt{2}$ times larger than the inter-clock comparison, because the CISC requires twice the time to obtain the same number of samples by switching between two states. What is more, CISC has about twice the instability of the inter-clock comparison without the switching states given by the blue dotted line in Fig. 2(a), which is the result of a smaller duty ratio leading to a more significant Dick effect. This can also be explained by the contribution of two identical clocks which have the same instabilities, and both contribute to half of the total instability. It is obvious that the inter-clock comparison will eventually increase due to the slowly frequency drift of the hydrogen maser. But CISC has a

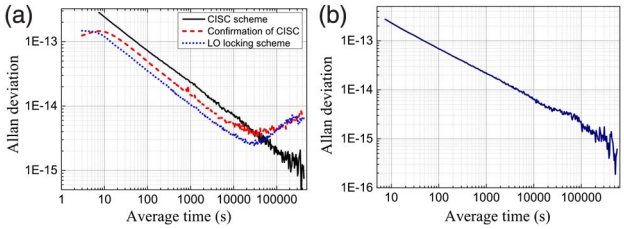

Fig. 2. (a) Confirmation of CISC method. The black solid line given by the result of CISC between two identical states has a 7.2×10^{-13} $\tau^{-1/2}$ dependence. It is twice that of the LO locking depicted by the blue dotted line, which is measured by comparison with a hydrogen maser. The red dashed line is the CISC scheme confirmed by a comparison with the same hydrogen maser. (b) Allan deviation of y_2-y_1 given as the uncertainty for the collisional frequency shifts.

$\tau^{-1/2}$ dependence indicated by the black solid line in Fig. 2(a) because CISC is unrelated to the hydrogen maser, and the RWFM and FFM are cancelled out by the closely switching states. Thereby, the CISC is able to break the limit set by inter-clock comparison and reach a lower instability.

The difference between the two identical states of the ^{87}Rb atomic fountain in CISC gives a 6.8×10^{-16} relative frequency bias reflecting the influence of the residual frequency drift (RFD)[19,20]. Basically, the output frequency of the LO would have a positive (negative) drift between two adjacent feedbacks such that the LO frequency is generally higher (lower) in the second state in CISC. This drift would be included in the error signals after interrogation. Theoretically, the bias is fixed at kT_c if the LO is assumed to have a constant drifting rate with $y = kt$ between adjacent feedbacks, where k is the relative drift rate. Then this model would give rise to a 6.2×10^{-16} systematic bias, which is inconsistent with the experiments above. But if the LO is not drifting at a constant rate, extra consideration should be taken into account to correct the systematic bias. Although effects other than LO drifting also change with time, for example the temperature of a fountain may fluctuate so that the black body radiation shifts and the cavity pulling shifts are different in two clock states; these changes are small within one CISC cycle. By means of the close switching in the CISC method, the time interval between the two samples is typically 3.7 s in our fountain; the change of temperature and many other parameters are minimal. Shifts like cavity pulling generated by these changes would vanish in the CISC after the averaging of samples in one day because of the closely interleaved switching states. In that way, the method is advantageous in reducing the effect, except for the one of interest.

One application of CISC is the measurement of the light shift in the atomic fountain clock. By inserting a computer controlled optical switch at the main optical path after the master laser, the CISC is applied to switch the fountain between two states, where the fountain is blocked or suffered from any potential stray light during the Ramsey interrogation. The error signals y_1 come from the state affected by stray light, and the error signals y_2 come from state unaffected by stray light. The differential error signals y_2-y_1 reflect the effect of interest, namely the light shift here, and most other effects would vanish after averaging. After the RFDs are subtracted from the corresponding measurements for each period of time, the evaluated light shifts are decoupled from the LO drifting as shown in Table 1. After several days of repeated comparison, the consistent results shown in Table 1 indicate that there are no visible effects of the light shift in the fountain. After proper correction, the light shift in Table 1 would sum up to give a zero relative frequency shift with a 2.1×10^{-15} uncertainty. The results show that no light shift is observed within this uncertainty.

Another application of CISC is the evaluation of the cold collisional frequency shift of ^{87}Rb atoms. It has been

Table 1. Comparison at Different Periods of Time for Light Shift ($\times 10^{-15}$)

Time (MJD)	y_1	y_2	RFD	Corrected y_2-y_1
57343-57344	1.32	−3.02	0.61	−3.73
57344-57346	1.24	1.81	0.55	1.12
57346-57350	1.29	1.40	0.58	0.69
57350-57351	0.76	0.80	0.34	0.38

confirmed that the collisional frequency shift of ^{87}Rb is about 50 times smaller than ^{133}Cs[3,4]. At the SIOM, this shift could be easily obtained using the CISC method to switch the fountain between a high atom density state and a low atom density state. The atom density is controlled by the microwave power in the state-selection cavity. Under different microwave powers, a different number of atoms are transferred from the $|F = 2, m_f = 0\rangle$ state to the $|F = 1, m_f = 0\rangle$ state. After pushing away all the atoms except those in the $|F = 1, m_f = 0\rangle$ state, atom clouds with different densities are subject to the Ramsey interrogation. As in the procedure in the evaluation of light shifts, RFDs are calculated and removed so that the results are only affected by the cold collisional shift. It is notable in Table 2 that measurements from different periods of time are inconsistent with each other, and all the results can combine to give a -2.2×10^{-15} relative frequency shift between two atom density states. The uncertainty given by the Allan deviation shown in Fig. 2(b) is 9.5×10^{-16}. Meanwhile, the fitting of time of the flight signal gives the detected size of the atom cloud and atom number so that the detected atom cloud density is determined. Averaged by the atom trajectory when atom cloud expansion is considered, the high atom density is approximately 1.2×10^7 cm^{-3}, which corresponds to a cold collisional frequency shift of several parts in 1×10^{17}, according to the measurement of Laboratoire National de Métrologie et d'Essais–Systèmes de Référence Temps-Espace (LNE-SYRTE) [3]. The main reason for the discrepancy may be ascribed to the microwave power dependent frequency shifts coupled with the cold collisional shift in the fountain, because the microwave power indeed switched in this scheme. Although more efforts might be necessary for us to separate these effects, the results show that CISC holds the potential to reach better evaluation uncertainties than that of inter-clock comparison.

Table 2. Comparison at Different Periods of Time for Cold Collisional Shift ($\times 10^{-15}$)

Time (MJD)	y_1	y_2	RFD	Corrected y_2-y_1
56840-56861	1.02	−2.33	0.44	−2.91
57121-57135	0.75	−1.82	0.31	−2.26
57278-57283	1.54	−1.50	0.66	−2.38

In conclusion, we present a CISC method which is able to remove the long-term drifts and potential non-white noise. A fountain working in the CISC scheme can be viewed as two clocks; thereby, the comparison reflects the innate difference due to the state switching. It has been proved by the comparison between identical states that the Allan deviation has a $\tau^{-1/2}$ dependence as predicted by the theory; although the comparison between the fountain and the hydrogen maser may have a $\tau^{-1/2}$ dependence at the averaging time of longer than 1×10^4 s. Moreover, the method is applied to the evaluation of the light shift, and no observable frequency shift is discovered within the 2.1×10^{-15} uncertainty. As another application of CISC, the cold collisional shift of ^{87}Rb is estimated to be around -2.2×10^{-15} with a 9.5×10^{-16} uncertainty. The results demonstrate that the CISC is powerful in the evaluation of ultra-small effects.

This work was supported by the National Natural Science Foundation of China under Grant Nos. 61275204 and 91336105.

References

1. J. Guena, M. Abgrall, A. Clairon, and S. Bize, Metrologia **51**, 108 (2014).
2. S. Peil, J. L. Hanssen, T. B. Swanson, J. Taylor, and C. R. Ekstrom, Metrologia **51**, 263 (2014).
3. Y. Sortais, S. Bize, C. Nicolas, and A. Clairon, Phys. Rev. Lett. **85**, 3117 (2000).
4. C. Fertig and K. Gibble, Phys. Rev. Lett. **85**, 1622 (2000).
5. T. P. Heavner, E. A. Donley, F. Levi, G. Costanzo, T. E. Parker, J. H. Shirley, N. Ashby, S. Barlow, and S. R. Jefferts, Metrologia **51**, 174 (2014).
6. B. J. Bloom, T. L. Nicholson, J. R. Williams, S. L. Campbell, M. Bishof, X. Zhang, W. Zhang, S. L. Bromley, and J. Ye, Nature **506**, 71 (2014).
7. N. Hinkley, J. A. Sherman, N. B. Phillips, M. Schioppo, N. D. Lemke, K. Beloy, M. Pizzocaro, C. W. Oates, and A. D. Ludlow, Science **341**, 1215 (2013).
8. C. W. Chou, D. B. Hume, J. C. J. Koelemeij, D. J. Wineland, and T. Rosenband, Phys. Rev. Lett. **104**, 070802 (2010).
9. Y. Ovchinnikov and G. Marra, Metrologia **48**, 87 (2011).
10. F. Fang, M. Li, P. Lin, W. Chen, N. Liu, Y. Lin, P. Wang, K. Liu, R. Suo, and T. Li, Metrologia **52**, 454 (2015).
11. M. M. Boyd, A. D. Ludlow, S. Blatt, S. M. Foreman, T. Ido, T. Zelevinsky, and J. Ye, Phys. Rev. Lett. **98**, 083002 (2007).
12. T. L. Nicholson, M. J. Martin, J. R. Williams, B. J. Bloom, M. Bishof, M. D. Swallows, S. L. Campbell, and J. Ye, Phys. Rev. Lett. **109**, 230801 (2012).
13. Y. Y. Jiang, A. D. Ludlow, N. D. Lemke, R. W. Fox, J. A. Sherman, L.-S. Ma, and C. W. Oates, Nat. Photon. **5**, 158 (2011).
14. C. Hagemann, C. Grebing, T. Kessler, S. Falke, N. Lemke, C. Lisdat, H. Schnatz, F. Riehle, and U. Sterr, IEEE Trans. Instrum. Meas. **62**, 1556 (2013).
15. S. Falke, H. Schnatz, J. S. R. V. Winfred, T. Middelmann, S. Vogt, S. Weyers, B. Lipphardt, G. Grosche, F. Riehle, U. Sterr, and C. Lisdat, Metrologia **48**, 399 (2011).

16. C. Degenhardt, H. Stoehr, U. Sterr, and F. Riehle, Phys. Rev. A **70**, 023414 (2004).
17. F. Riehle, *Frequency Standards: Basics and Applications* (Wiley-VCH, 2005).
18. C. Shi, R. Wei, Z. Zhou, T. Li, L. Li, and Y. Wang, in *Joint Conference of the IEEE International Frequency Control and the European Frequency and Time Forum* (2011).
19. Y. Du, R. Wei, R. Dong, F. Zou, and Y. Wang, in *Joint Conference of the IEEE International Frequency Control Symposium & the European Frequency and Time Forum* (2015).
20. Y. Du, R. Wei, R. Dong, F. Zou, J. Lin, W. Wang, and Y. Wang, Chin. Opt. Lett. **13**, 091201 (2015).
21. C. Shi, R. Wei, Z. Zhou, D. Lu, T. Li, and Y. Wang, Chin. Opt. Lett. **8**, 549 (2010).